Earliest siphuncle-bearing cephalopod from the early Cambrian

https://doi.org/10.1038/s41586-026-10868-y

Received: 8 February 2026

Accepted: 30 June 2026

Published online: 29 July 2026

Check for updates

Zuchen Song (宋祖晨)[1], Bing Pan (潘兵)[2], Junfeng Guo (郭俊锋)[1,3]✉, Jakob Vinther[4]✉, Guoxiang Li (李国祥)[2], Jian Han (韩健)[3], Heyo Van Iten[5,6], Xiaofang Zhao (赵晓芳)[1], Xianzhi Pei (裴先治)[1], Jiaxin Peng (彭佳欣)[1], Yaqin Qiang (强亚琴)[7], Boyao Zhang (张博耀)[1] & Hanjie Wen (温汉捷)[1,8]✉

Modern cephalopods are unique among molluscs in ancestrally possessing a chambered, gas- and fluid-filled shell, the internal septa of which are penetrated by a siphuncle. Combined with jet propulsion, the siphuncle enables cephalopods to engage in a nektonic and mostly predatory lifestyle through long-term regulation of their bouyancy[1]. The origin of this key innovation remains unknown, as major gaps exist between the earliest accepted cephalopod, *Plectronoceras cambria*[2] from the late Cambrian era, and molecular clock estimates placing the divergence of the lineage from other molluscs in the early Cambrian[3,4]. Here we report *Eoceras shaanxiense* gen. et sp. nov., a millimetre-sized cephalopod with an orthoconic shell from the Shuijingtuo Formation (Cambrian Stage 3) of South China. Internally, the shell exhibits multiple septa along with a peripherally situated segmented tube that appears to bridge the septa through minute canals, indicating that the soft body migrated aperturally to form successive chambers during growth while maintaining contact with earlier chambers via the tube. Collectively, these features identify the segmented tube in *E. shaanxiense* gen. et sp. nov. as a candidate primordial cephalopod siphuncle, thus extending the known range of stem cephalopods back to the early Cambrian and revealing the early stages in the evolutionary assembly of a chambered phragmocone employed in buoyancy regulation.

Cephalopoda, comprising the squids, cuttlefish, octopuses and *Nautilus*, includes the most intelligent invertebrate animals and has undergone substantial modifications of the ancestral body plan during the course of its long Phanerozoic history[1,5]. The appearance of the chambered shell, with the chambers (camerae) interconnected by a vascularized siphuncle for regulating long-term buoyancy, along with subsequent evolutionary modifications to this apparatus, enabled cephalopods to become agile nektonic predators exploiting a wide range of marine habitats[1,6,7]. Most extant cephalopods belong to coleoids, in which the endocochleate phragmocone has often been reduced or lost in lieu of evolving novel, chemically mediated buoyancy mechanisms[1]. Conversely, in Palaeozoic ectocochleate forms, the phragmocone underwent significant transitions in morphology and function. Early innovations such as shell coiling, formation of cameral deposits and substantial increase in total body size were crucial steps leading to the first major radiation of cephalopods during the Great Ordovician Biodiversification Event[8–11].

Together with embryological data obtained from modern cephalopods[12], evidence from the fossil record suggests that the first cephalopods evolved during the Cambrian Explosion (560–520 million years ago (Ma)) from benthic, low-conical (that is, monoplacophoran-like) molluscs, and gradually became increasingly elongated dorsally[1,6,13–15]. Several Cambrian taxa preceding *P. cambria* have been considered candidate cephalopod ancestors, including *Knightoconus*[13], *Yochelcionella*[16], *Helcionella*[6], *Tannuella*[16,17] and *Turcutheca*[18]. A specific hypothesis derives cephalopods from circothecid hyoliths[18,19], although the monophyly of hyoliths and their relationship to molluscs remains debated[20–23]. Nonetheless, how a simple conical shell with septa evolved into a chambered buoyancy apparatus remains unresolved owing to the significant gaps in the fossil record between the relatively complex siphunculate cephalopods known from the late Cambrian and the current lack of older unequivocal records of intermediate forms[7,8].

During the Cambrian Explosion, fossils recorded in several unique taphonomic windows, demonstrate the apparent first appearances of nearly all skeletonized metazoan phyla[24]. Specifically, the early Cambrian fossil record integrated with molecular clock analyses reveal that molluscs, including lineages to all extant conchiferan classes, originated and diversified rapidly during this interval[3,25,26]. Unequivocal stem cephalopods, however, have long appeared to be absent from this crucial early to middle Cambrian interval. This creates a substantial

---

[1] Key Laboratory of Western China's Mineral Resources and Geological Engineering, Ministry of Education, School of Earth Science and Resources, Chang'an University, Xi'an, China. [2] State Key Laboratory of Palaeobiology and Stratigraphy, Nanjing Institute of Geology and Palaeontology, Chinese Academy of Sciences, Nanjing, China. [3] State Key Laboratory of Continental Evolution and Early Life, Shaanxi Key Laboratory of Early Life and Environments, Department of Geology, Northwest University, Xi'an, China. [4] School of Earth Sciences, Life Sciences Building, University of Bristol, Bristol, UK. [5] Department of Geology, Hanover College, Hanover, IN, USA. [6] Department of Invertebrate Paleontology, Cincinnati Museum Center, Cincinnati, OH, USA. [7] Geological Hazards Prevention Institute, Gansu Academy of Sciences, Lanzhou, China. [8] College of Earth and Planetary Sciences, University of Chinese Academy of Sciences, Beijing, China. ✉e-mail: junfengg@chd.edu.cn; Jakob.Vinther@bristol.ac.uk; wenhanjie@vip.gyig.ac.cn

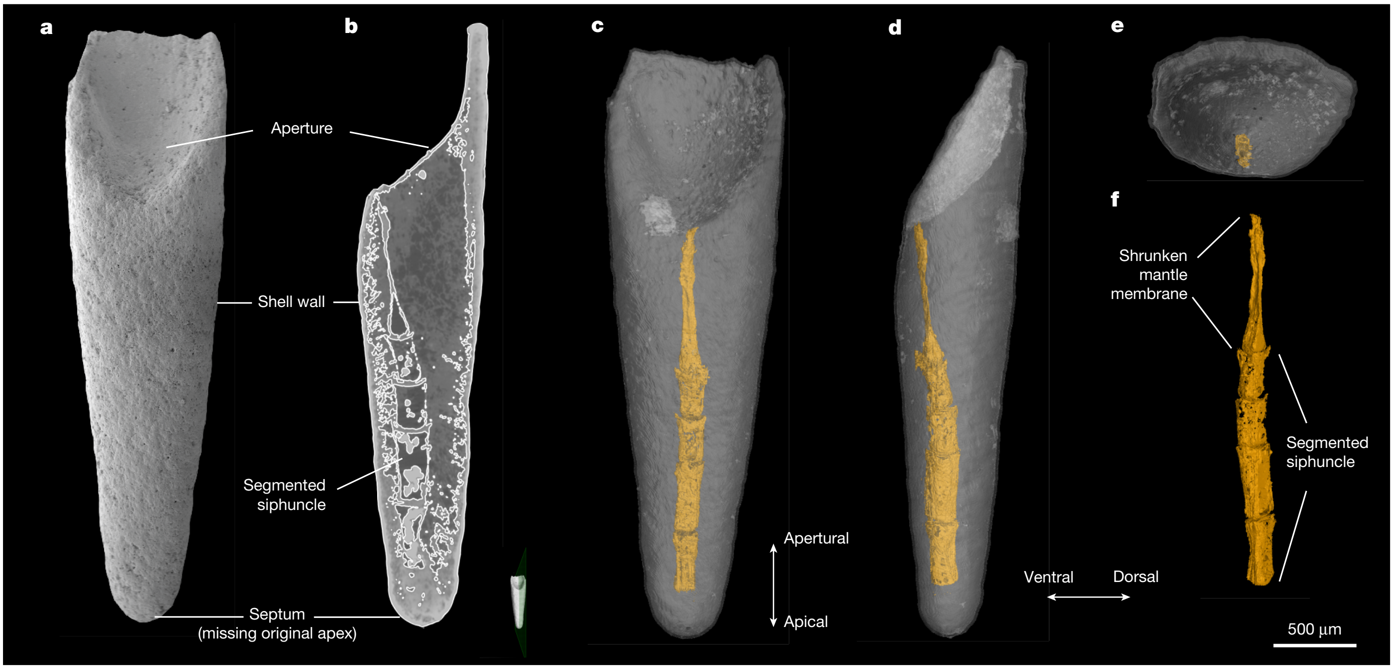

Fig. 1 | SEM and micro-CT images of the phragmocone and siphuncle of *E. shaanxiense* gen. et sp. nov. (CUBar297-1 holotype). **a**, SEM image. Ventral view of a secondarily phosphatized orthoconic shell with an exposed septum (original apical portion of the shell not preserved) and a strongly oblique open aperture. **b**, Micro-CT image. Lateral view of a camerate shell preserving the segmented siphuncle. Light greyscale values correspond to high X-ray attenuation and represent original biological structures with secondary phosphatization or phosphatized infillings (intermediate grey values). Dark greyscale values indicate void spaces. **c**, Rendered micro-CT image, ventral view, showing the siphuncle (yellow) extending towards the aperture. **d**,**e**, Rendered micro-CT images. Lateral (**d**) and apertural (**e**) views showing the siphuncle situated close to the ventral side of the phragmocone. **f**, Rendered micro-CT image of an isolated siphuncle with a secondarily shrunken, last formed (apertural-most) segment connected to four earlier formed segments. No internal septa are preserved.

temporal gap before their first appearance in the fossil record in the late Cambrian, represented by *P. cambria*[2].

Here we present millimetric, orthoconic, camerate shells (Fig. 1) from phosphatic carbonates in the early Cambrian Shuijingtuo Formation of southern Shaanxi, South China (Extended Data Figs. 1 and 2). These tubular small shelly fossils (SSFs), which have lengths of 2 to 4 mm, are assigned to a new genus *Eoceras*. Scanning electron microscopy (SEM) and micro-computed tomography (micro-CT) reveal the presence of an internal tube, segmented by multiple transverse septa within the shell cavity. This segmented tube, displaced toward one side of the outer shell, is interpreted as a siphuncle—homologous to that of living cephalopods. This key diagnostic feature of *E. shaanxiense* gen. et sp. nov., therefore, suggests that stem cephalopods with core components of their unique buoyancy apparatus were in fact present in the early Cambrian, extending the known fossil record of the lineage back to approximately 520 Ma and corroborating molecular clock estimates of the timing of cephalopod origins[1,3,4].

Available material of *E. shaanxiense* gen. et sp. nov. ($n = 32$) can be categorized into three general taphonomic types (Types I–III) (Figs. 1 and 2). As revealed using micro-CT imaging, Type I specimens (Figs. 1 and 2a–e) preserve the conical outer shell (phragmocone) as well as the internal, peripherally situated, segmented siphuncle (Fig. 1, Extended Data Fig. 3 and Supplementary Video 1). The shells range from 1.5–4.4 mm in length and 0.6–1.0 mm in maximum diameter, and expand adaperturally at 8–15° (Extended Data Table 1). The segmented tubes range in diameter from 0.3 to 0.7 times that of the enclosing outer shells, which have undergone secondary phosphatization of original shell material along with partial infill. The bluntly conical apical end of Type I specimens is not the original, embryonic apex of the shell but rather an exposed septum. At the opposite end of the shell, the margin of the aperture runs obliquely to the long axis of the shell (Figs. 2a–e and 3h). No opercula were found in association with these or other specimens.

Type II specimens (Fig. 2f–j) consist of phragmocones that have been broken or abraded to reveal the secondary septa and several, regularly spaced internal chambers of the siphuncular segments. Such specimens consist primarily of diagenetic secondary phosphatic infillings acting as steinkern of the septa and mouldic linings onto the inner surface of the phragmocones. Shells with length 2–3 mm exhibit 4–6 septa, whereas shells with length of less than 2 mm exhibit only 1–2 septa (including the exposed apical septum) (Figs. 2f–j and 3a,b,d,j and Extended Data Table 1), revealing some ontogenetic aspects.

Type III specimens (Fig. 2k–o) consist of phosphatic steinkerns of the siphuncle, including its flaring apertural-most unit, representing a lining that occupies most of the body chamber inside which the animal was situated. No mineralized features interpretable as endosiphuncular deposits[27], such as those present in younger Paleozoic cephalopods, were observed. The surface of the tubular steinkerns exhibits fine traces of the interior margins of multiple septa as indentations (Fig. 2m–p), corresponding in spacing to the secondarily thickened septa seen in Type II specimens. The chamber nearest to the aperture (body chamber) contains an internal membrane that forms an expansive, torch-shaped structure tapering into the siphuncle (Fig. 2k–m,o and Extended Data Fig. 4), a feature also consistent with Type I specimens (Extended Data Fig. 3). The wall of the siphuncle varies in shape among specimens (Fig. 2k–m,o and Extended Data Fig. 4a–e), suggesting that it was originally organic or only weakly mineralized, allowing its diameter to vary in life or post mortem.

Examination of the microstructure, ornamentation and preservation of all specimens revealed additional details of the anatomy of the phragmocone, siphuncle and septa. Some Type I specimens with broken shell reveal that the outer shell wall, which is approximately 0.07 mm

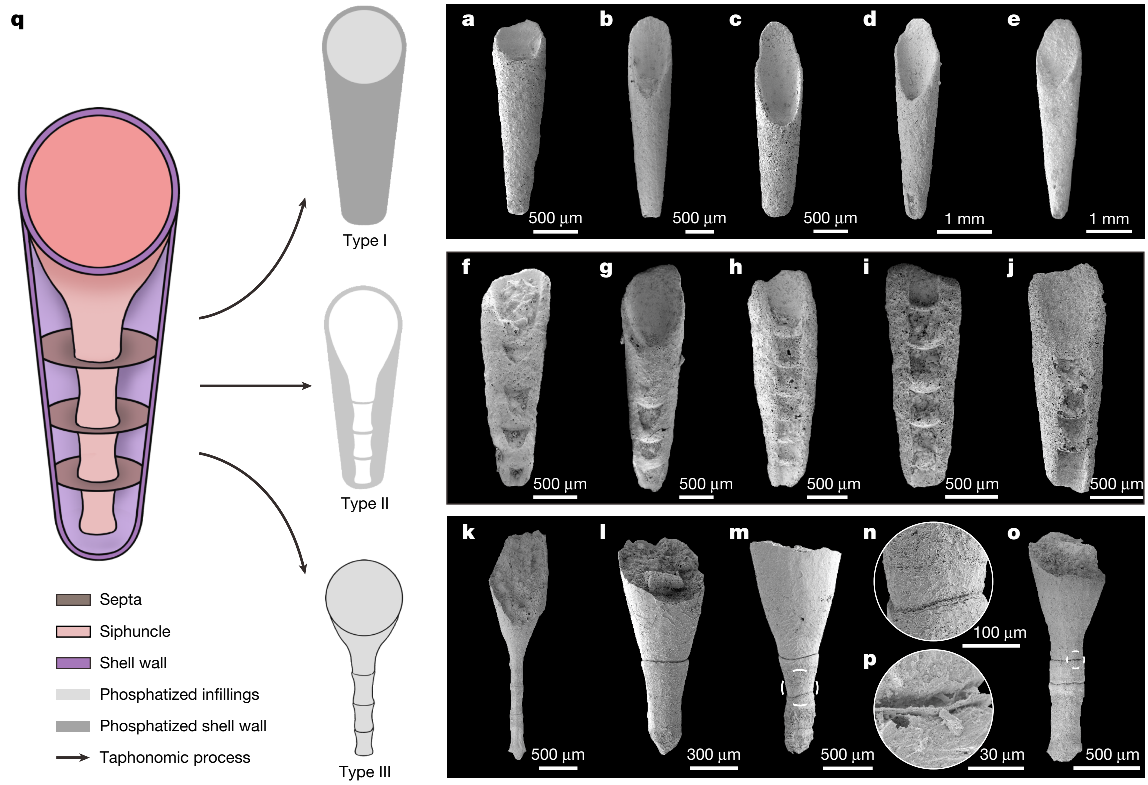

Fig. 2 | Preservation types of *E. shaanxiense* gen. et sp. nov. from the Cambrian Shuijingtuo Formation, South China. a–e, Type I preservation; specimens CUBar335-15 (**a**), CUBar297-4 (**b**), CUBar298-5 (**c**), CUBar337 -7 (**d**) and CUBar335-1 (**e**), consisting of secondarily phosphatized orthoconic phragmocones. **f–j**, Type II preservation; specimens CUBar293-3 (**f**), CUBar297-8 (**g**), CUBar297-10 (**h**), CUBar297-19 (**i**) and CUBar298-20 (**j**), consisting of broken ventral phragmocones with phosphatized infillings of the camerae and exposed 'septa' that formed by secondarily infilling and thickening of the cavities between adjacent siphuncular segments. **k–m**,**o**, Type III preservation; specimens CUBar335-1 (**k**), CUBar299-17 (**l**), CUBar299-30 (**m**) and CUBar335-16 (**o**), consisting of the isolated and expanded apertural-most segment and preceding siphuncular segments. **n**,**p**, Close-ups of the circled areas in **m** (**n**) and **o** (**p**), showing details of the junctions of the siphuncle with the innermost portions of the relic thin septa. **q**, Illustration of Type I, II and II specimens.

thick, consists of three distinct layers: an outer layer ornamented with fine, external annulations that represent growth lines (Fig. 3a,i,l,m and Extended Data Fig. 5); a smooth inner layer (Fig. 3i,l); and an intervening layer containing poorly preserved fibrous bundles (Fig. 3d,j,k), possibly similar to the prismatic layer of ectocochleate cephalopods. In specimens preserving the oblique apertural margin, growth lines adjacent to this margin run parallel to it (Extended Data Fig. 5), whereas growth lines elsewhere on the outer shell are transverse (Fig. 3m). This pattern demonstrates an ontogenetic change in apertural morphology during growth and how the organism interacted with its external environment upon maturity. Unlike the outer shell, the wall of the segmented tube consists of a single thin layer with no original microstructure being preserved (Fig. 3d,e,g,h and Extended Data Fig. 3b,c,f,g). The clear differences in composition between the outer shell and siphuncle suggest that the former was secreted by the mantle epithelium and mineralized, while the latter was organic and more plastic in morphology during ontogeny and post mortem. Notably, the apical-most septum, preserved in many specimens (Fig. 3a,b,d,f and Extended Data Fig. 3g), is similar to all other septa in morphology, being flat near its margins and showing an abrupt transition into the concave central portion. We therefore interpret the blunt apex as an exposed septum, as the result of loss of more apical portions of the shell, including the original embryonic apex either during ontogeny, or alternatively post mortem. Isolated septa recovered from phosphatic residues (Extended Data Fig. 6) preserve columnar zones along their margins, together with radial canal structures (Fig. 3b,c), which are similar in size, shape and position to those of septa preserved in situ. The canals at the periphery of the septa, preserve as pits on the convex surface (Extended Data Fig. 6c,d) corresponding with hollow tubes of the inner side (Extended Data Fig. 6e,f). The diameter of individual canal is around 5 µm. Isolated septa are very thin and semi-transparent under optical light (Extended Data Fig. 6a,b), reflecting their delicate, membranous nature within the shell in vivo.

Cephalopod affinity of *Eoceras* gen. nov.

E. shaanxiense gen. et sp. nov. exhibit a number of features suggesting homology with the phragmocone, septa and siphuncle of known cephalopods, specifically orthoconic ellesmerocerid cephalopods[28], such as *Paleoceras*, with a ventrally displaced and less specialized siphuncle. However, *E. shaanxiense* gen. et sp. nov. lacks septal foramina and associated septal necks or connecting rings, exhibiting instead a continous septal membrane which divides the siphuncle into segments. The anatomy of *E. shaanxiense* gen. et sp. nov. exhibit many of the key inferred conditions proposed for the ancestral cephalopod[7,8,19,29]. These include a steeply conical, septate external shell with an aperturally expanding body chamber and a ventrally displaced, segmented siphuncle that was organic or weakly mineralized (Fig. 4a). Given that cephalopods may have evolved from monoplacophoran-like molluscs that modified the original body axes through dorsal elongation[1], we use the unambiguous orientation terminology 'apertural/apical' and define 'ventral/dorsal' mainly on the basis of peripherally situated siphuncle and the oblique apertural margin.

Several additional Cambrian taxa have been interpreted as possible stem cephalopods. However, all these fossils are either not molluscs or lack the full suite of anatomical structures exhibited by *E. shaanxiense* gen. et sp. nov. and other cephalopods. For example, even though the

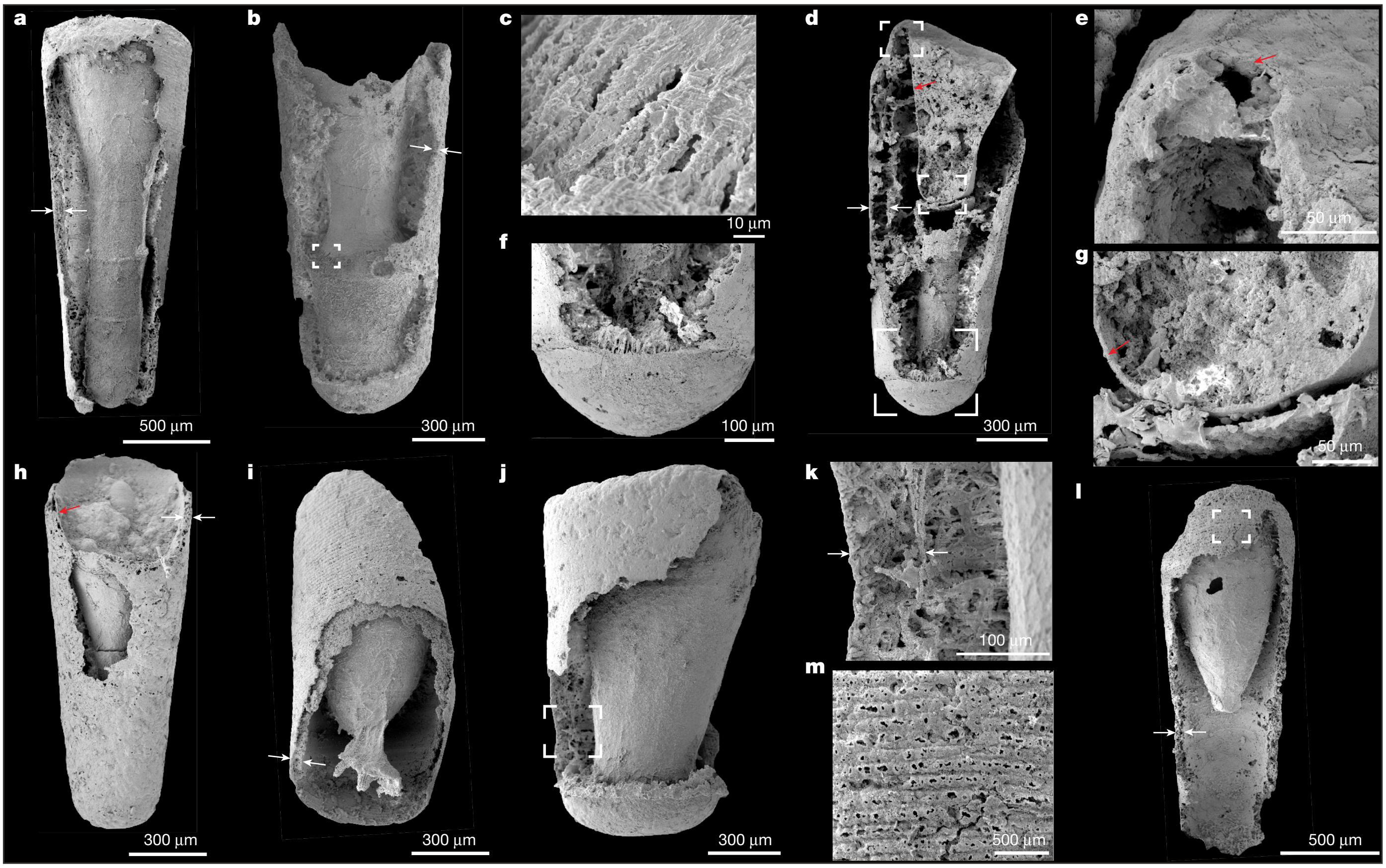

Fig. 3 | Anatomy of *E. shaanxiense* gen. et sp. nov. a, CUBar293-2. Dorsal view of a broken shell preserving the siphuncle. **b**, CUBar301-41. Dorsal view of a broken shell terminating in an exposed septum and preserving a single internal septum joined to the ends of two adjacent segments of the partial siphuncle. **c**, Close-up of the boxed area in **b**, showing the minute canals connecting the siphuncle to the septum. **d**–**g**, CUBar297-12. **d**, Ventral view of a broken shell preserving the adapertually flaring mantle membrane narrowing into the siphuncle (upper end of the specimen) and additional adapical siphuncular segments. **e**, Close-up of the top box in **d**, showing the gap between the shell and the mantle membrane. **f**, Close-up of the bottom box in **d**, showing the apical end of the phragmocone truncated at a septum. **g**, Close-up of the middle box in **d**, showing the gap where a septum is missing between adjacent segments of the siphuncle. **h**, CUBar299-6. Ventral view of a broken camerate shell revealing the siphuncle. **i**, CUBar299-2. Lateral view, showing the three-layered wall of the phragmocone, part of the siphuncle, and faint transverse ornamentation (accretionary growth lines). **j**,**k**, CUBar300-2. **j**, Dorsal view of a shell that has been truncated near its apical end. **k**, Close-up of the box in **j**, showing the three-layered wall of the phragmocone preserving relic fibrous bundles (secondarily phosphatized, originally aragonitic prismatic microstructure). **l**,**m**, CUBar300-9. **l**, Dorsal view of a chambered shell preserving portions of the flaring mantle membrane towards the aperture and the inner smooth layer of the phragmocone wall. **m**, Close-up of the box in **l**, showing closely spaced, parallel transverse growth lines on the outer layer of the phragmocone. White arrows mark the three-layered wall of the phragmocone; red arrows indicate the single-layered wall (or membrane) of the siphuncle and mantle.

helcionellid *Tannuella* from the early Cambrian of South Australia and Siberia[1,17,26] and the hypseloconid *Knightoconus* from the late Cambrian of Antarctica[13] possess a septate shell, the absence of a diagnostic siphuncle obscures their precise phylogenetic position within or outside total-group Cephalopoda. Nevertheless, an affinity with the stem cephalopods cannot be refuted outright for any of these taxa, provided that the evolution of a camerate shell preceded that of the siphuncle. An unnamed early Cambrian taxon from eastern Newfoundland with a putative siphuncle in a peripheral position[30] has been reinterpreted as a taxonomic chimera[31]. Finally, *Nectocaris pteryx*, a shell-less species from the early Cambrian Chengjiang biota and middle Cambrian Burgess Shale[32], lacks definite molluscan characters[1] and has been reinterpreted as a stem chaetognath[33].

As described above, the siphuncle and septa of *E. shaanxiense* gen. et sp. nov. are interconnected by minute canals extending from the central portions of the septa into the outer wall of the siphuncle (Fig. 3b,c and Extended Data Fig. 6g,h). Although different from later cephalopods, in which the siphuncle passes through the septa via the septal foramina[34], the minute canals of *E. shaanxiense* gen. et sp. nov. could have permitted fluid transfer between the columnar zone of the septa and the siphuncle (Fig. 4a). Moreover, the extremely thin central portion of the septa (specimen BM-05; Extended Data Fig. 6a,b) may have facilitated permeability, allowing additional fluid transfer by osmosis (Fig. 4a). In brief, *E. shaanxiense* gen. et sp. nov. exhibits internal shell structures suggesting that the living animal could have been able to regulate (to some degree) its own buoyancy. Additionally, the exposed apical end of *E. shaanxiense* gen. et sp. nov., truncated to expose a septum, is reminiscent of Ordovician–Silurian Ascocerida (subclass Nautiloidea)[1,35]. Although this comparison has no phylogenetic significance, it may attest to structural and developmental similarities in how the phragmocone could be modified during ontogeny. Together, the gross anatomical and microstructural features described above support the interpretation of *E. shaanxiense* gen. et sp. nov. as a primitive, stem-group cephalopod (Fig. 4b).

Orthoconic shell origin of cephalopods

Palaeontological data provide the most direct evidence bearing on the origin and early evolution of higher taxa. In the case of cephalopods, the appearance of a chambered shell connected by a siphuncle was

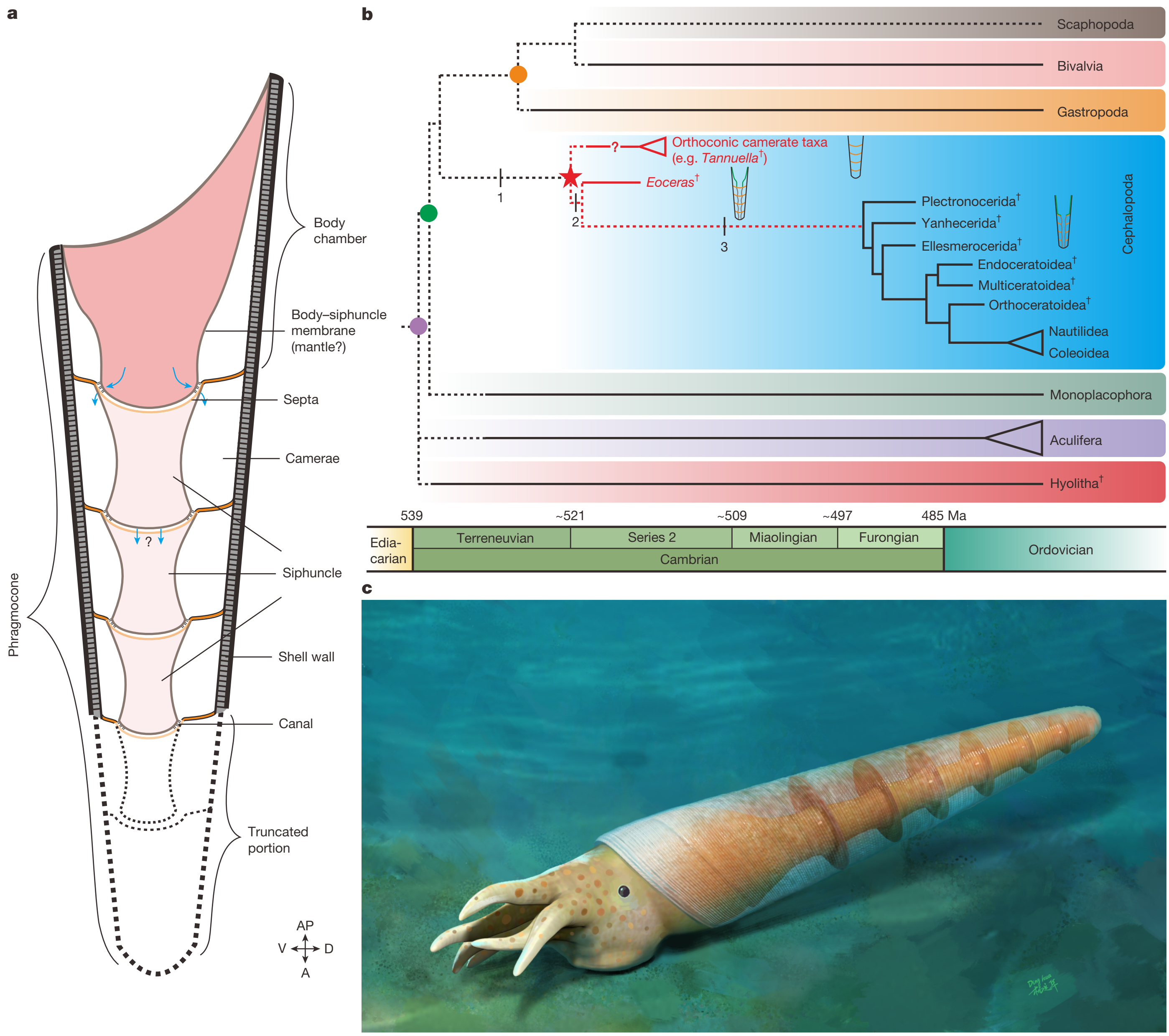
a
Body chamber
Body–siphuncle membrane (mantle?)
Septa
Camerae
Siphuncle
Shell wall
Canal
Truncated portion
Phragmocone
?
AP
V
D
A
b
Scaphopoda
Bivalvia
Gastropoda
Orthoconic camerate taxa (e.g. Tannuella†)
?
Eoceras†
1
2
3
Plectronocerida†
Yanhecerida†
Ellesmerocerida†
Endoceratoidea†
Multiceratoidea†
Orthoceratoidea†
Nautilidea
Coleoidea
Cephalopoda
Monoplacophora
Aculifera
Hyolitha†
539
~521
~509
~497
485 Ma
Edia-carian
Terreneuvian
Series 2
Miaolingian
Furongian
Cambrian
Ordovician
c

Fig. 4 | Schematic tangential cross-section, hypothesized phylogenetic position and life reconstruction of *E. shaanxiense* gen. et sp. nov. **a**, Tangential cross-section through an apically truncated shell, showing the internal anatomy. AP, apertural; A, apical; D, dorsal; V, ventral. **b**, Phylogenetic hypothesis showing *E. shaanxiense* gen. et sp. nov. as a stem-group cephalopod that appeared no later than about 520 Ma. Purple circle, total-group Mollusca[3,23]; green circle, total-group Conchifera; orange circle, total-group Diasoma[4]; red star, total-group Cephalopoda[1,11]. Dotted lines indicate clade divergence times inferred from phylogenomic data[3,4] and inferred ghost lineages; solid lines indicate earliest fossil occurrences. Numbers denote the following key steps: (1) orthoconic shell with imperforate septa (limited osmoregulation); (2) septal thinness and development of segmented siphuncle that bridges septa through minute canals; (3) septal foramen and development of septal necks and true connecting rings. Dagger symbols denote fossils. **c**, Life reconstruction of *E. shaanxiense* gen. et sp. nov.; artwork by Dinghua Yang. The anatomy of the soft body extending beyond the shell aperture is conjectural.

a key evolutionary innovation[7]. *E. shaanxiense* gen. et sp. nov., now probably the earliest known fossil cephalopod, was very small and orthoconic, suggesting that the ancestral cephalopod was similar to it in size and shell shape.

The single-layered wall enveloping the body (mantle membrane) within the body chamber and apically transitioning into the siphuncle (Fig. 3a,b,d,h and Extended Data Figs. 3 and 4) must represent some membrane that enveloped the animal forming some extracellular component of the mantle. Given its natural transition into the siphuncle, it appears that the mantle and siphuncle tissues were less differentiated than those in living nautilus[36]. The cellular tissue associated with the preserved mantle membrane must have secreted both the shell wall, the septa, and condensing to form the siphuncle during growth.

In modern cephalopods, liquid and gas exchange between the camerae occurs via a porous connecting ring and contraction of the siphuncle cord[37]. In *E. shaanxiense* gen. et sp. nov., osmoregulation would have taken place via the siphuncle, which is connected by the septal canal structures potentially homologous to that of the connecting ring associated with the septal neck in later cephalopods[38,39], and possibly also via permeable septal membranes.

Together with *P. cambria* and older camerate shells lacking a siphuncle, *E. shaanxiense* gen. et sp. nov. (Cambrian Stage 3) may represent a crucial intermediate form for understanding key steps in the evolution of cephalopods (Fig. 4b) given the presence of a siphuncle, yet complete membranous septa connected by delicate canals. The initial stages of cephalopod evolution, therefore, presumably involved the development of osmoregulation through thin septal membranes, which could be exemplified by orthoconic camerate taxa lacking a siphuncle, such as the slightly younger genus *Tannuella*[1,17,26] (Cambrian Stage 4 of Australia and Siberia). Other septate orthoconic fossils, such as *Cupitheca* cf. *C. mira* (Cambrian Stage 3 of Mexico)[40] and *Tchuranitheca* sp. (Cambrian Stage 3 of Siberia)[41], may also represent stem-group cephalopod members that evolved prior to the emergence of the siphuncle. Alternatively, these taxa may be rejected as potential cephalopod precursors on account of their relatively thick, two-layered septum, which may not have been capable of osmoregulation—although septal canals are also documented that may have served an osmoregulatory role[42].

Following the appearance of a functional siphuncle in *E. shaanxiense* gen. et sp. nov., subsequent cephalopod evolution recorded in the late Cambrian species *P. cambria* and the more derived ellesmerocerids, featured perforation of the septum for the through passage of the siphuncle as well as the development of septal necks and true connecting rings. Together, these innovations increased the efficiency of gas and fluid exchange between the living animal and the camerae. Notably, *E. shaanxiense* gen. et sp. nov. refutes a specific hypothesis for the origin of the siphuncle[7]. It has been suggested that the formation of a septal foramen along with septal necks/connecting rings allowed for the formation of an epithelial extension into the previously formed chambers becoming the siphuncle. Given the possession of a siphuncle but complete septa of *E. shaanxiense* gen. et sp. nov., the evolutionary polarization of key buoyancy-regulating elements in the cephalopod phragmocone can therefore be inferred.

Considering its very small body size, simpler system for osmotic fluid exchange, and relatively thick shell walls[43], *E. shaanxiense* gen. et sp. nov. may have had a mostly benthic mode of life (Fig. 4c), although the truncation of the embryonic shell would reduce energy consumption, improve mobility and increase buoyancy[35,42], which suggests an adaptive value of this feature for a swimming lifestyle. It is also possible that the small size of available specimens is a consequence of the preferential preservation of juvenile specimens in the SSF taphonomic window, as has been observed in other conchiferan taxa[44].

Future reassessment of tubular SSFs

SSFs display considerable morphological disparity and taxonomic diversity[24] and are central to understanding early metazoan evolution during the Cambrian Explosion. Tubular and cap-shaped metazoans, many with the earliest biomineralized skeletons, dominate SSF assemblages in pre-trilobite Cambrian strata[45]. Most of these taxa have been affiliated to lophotrochozoans[46], a major group that includes both molluscs and hyoliths. Indeed, the cephalopod *E. shaanxiense* gen. et sp. nov. bears some marked resemblance to hyoliths within the genus *Cupitheca*[42,44,47] in having an orthoconic or slightly cyrtoconic, septated shell and a truncated apex. Furthermore, we note that taxa referred to *Inflatatheca*[48] are very similar to *E. shaanxiense* gen. et sp. nov., preserved as steinkerns tapering into a tubular structure with at least one segment and may be the same taxon.

Although the affinities of hyoliths have been debated, they share unique shell microstructures with molluscs, suggestive of some close relationship[49]. One scenario could be that these comparable shell features evolved independently in hyoliths and cephalopods, but from a shared ancestral biomineralization pathway and a similarly organized shell secreting gland or mantle. Alternatively, hyoliths or certain members of this clade (*Cupitheca*), if polyphyletic, are stem cephalopods within crown Conchifera in which *E. shaanxiense* gen. et sp. nov. evolved from diminutive cupithecid molluscs exhibiting orthoconic, septate shells lacking a functional siphuncle. Future discoveries and anatomical studies may eventually resolve these competing scenarios or refute them both.

Systematic palaeontology

Phylum Mollusca Linnaeus, 1758
Class Cephalopoda Cuvier, 1797 (stem group)
Order and Family uncertain
Eoceras gen. nov. Song & Guo

Type species. *Eoceras shaanxiense* gen. et sp. nov. Song & Guo, by monotypy.
Diagnosis. As for type species, by monotypy.
Etymology. The generic name derives from the Greek *Eo*-, or dawn, and the Greek -*ceras*, or horn, indicating that the taxon is interpreted to be the earliest known, siphuncle-bearing cephalopod.

Eoceras shaanxiense gen. et sp. nov. Song & Guo

Holotype. Palaeontological collections of Chang'an University in Xi'an, Shaanxi Province, China CUBar297-1 (Fig. 1).
Referred material. Paratypes ($n = 7$): CUBar335-15 (Fig. 2a), CUBar297-4 (Fig. 2b), CUBar298-5 (Fig. 2c), CUBar337-7 (Fig. 2d), CUBar335-1 (Fig. 2e), CU(CT-Eoceras)-7 (Extended Data Fig. 3a–d) and CU(CT-Eoceras)-11 (Extended Data Fig. 3e–h).

Other specimens: broken ventral phragmocones ($n = 5$): CUBar293-3 (Fig. 2f), CUBar297-8 (Fig. 2g), CUBar297-10 (Fig. 2h), CUBar297-19 (Fig. 2i) and CUBar298-20 (Fig. 2j); isolated siphuncle ($n = 8$): CUBar335-1 (Fig. 2k), CUBar299-17 (Fig. 2l), CUBar299-30 (Fig. 2m,n), CUBar335-16 (Fig. 2o,p), CUBar299-9 (Extended Data Fig. 4a,b), CUBar335-17 (Extended Data Fig. 4c), CUBar299-25 (Extended Data Fig. 4d) and CUBar299-16 (Extended Data Fig. 4e); broken shell ($n = 7$): CUBar293-2 (Fig. 3a), CUBar301-41 (Fig. 3b), CUBar297-12 (Fig. 3d–g), CUBar299-6 (Fig. 3h), CUBar299-2 (Fig. 3i), CUBar300-2 (Fig. 3j,k) and CUBar300-9 (Fig. 3l,m and Extended Data Fig. 5a,b); isolated septa ($n = 4$): BM-05 (Extended Data Fig. 6a,b), CUBar301-3 (Extended Data Fig. 6c,d), CUBar336-16 (Extended Data Fig. 6e,f) and CUBar301-31 (Extended Data Fig. 6g,h).
Etymology. The species named after Shaanxi Province, China, the holotype locality.
Locality and horizon. Liaoyeba village, Gaoqiao town, Zhenba county, Shaanxi Province, China; Lower Shuijingtuo Formation, *Eoredlichia–Wutingaspis* Biozone (Cambrian Stage 3).
Diagnosis. Millimetric, orthoconic chambered shell with a highly oblique aperture and a bluntly conical, non-expanded apical end (secondarily exposed septum). Siphuncle wide, segmented, and displaced ventrally within the shell (as indicated by the orientation of the oblique aperture), with the juncture between each segment occupied by a transverse septum. Septa very thin, semi-transparent, consisting of a convex central part and a planar marginal portion harbouring radial internal tubules. Siphuncle is connected to the septum by minute canals on the transitional outer portions of the septa.
Comparisons. The orthoconic shell of *E. shaanxiense* gen. et sp. nov., particularly its blunt, conical apical end, closely resembles the shell of *Cupitheca mira*[48,50,51], an orthothecid hyolith from adjacent stratigraphic horizons. Additionally, the shell morphology of *E. shaanxiense* gen. et sp. nov. is similar to those of *Cupitheca* cf. *C. mira*[40] and *Tchuranitheca* sp.[41]. However, those hyolith taxa possess two-layered septa. *E. shaanxiense* gen. et sp. nov. differs substantially from *Cupitheca* and other hyoliths in possessing a siphuncle. There are distinct similarities between *E. shaanxiense* gen. et sp. nov. and specimens referred to as *Inflatatheca*[48] from the same deposit. These specimens preserve as steinkerns, tapering to form what appears to be the first segment of the siphuncle described here. It is therefore likely they

can be attributed to *E. shaanxiense* gen. et sp. nov. On the other hand, the type material of *Inflatatheca*[52] consists of three poorly preserved steinkerns lacking crucial features of the external shell, aperture or a segmented siphuncle. Ultimately, its gross morphology of the steinkern is insufficiently distinct from other well-known taxa, such as *Doliutheca*[53,54], which is clearly distinct from *E. shaanxiense* gen. et sp. nov. Given that is impossible to assign any fossil to this taxon with confidence, we consider *Inflatatheca* a nomen dubium. The cloudinid cnidarian *Mianxiantubus*[55] is readily distinguishable by being composed of stacked conical elements made out of the external shell, and not derived from subsequent internal formation of septa and a siphuncle as in *E. shaanxiense* gen. et sp. nov.

Online content

Any methods, additional references, Nature Portfolio reporting summaries, source data, extended data, supplementary information, acknowledgements, peer review information; details of author contributions and competing interests; and statements of data and code availability are available at https://doi.org/10.1038/s41586-026-10868-y.

1. Kröger, B., Vinther, J. & Fuchs, D. Cephalopod origin and evolution: a congruent picture emerging from fossils, development and molecules. *Bioessays* **33**, 602–613 (2011).
2. Walcott, C. D. Cambrian faunas of China. *Proc. US Natl Mus.* **29**, 1–106 (1905).
3. Kocot, K. M., Poustka, A. J., Stöger, I., Halanych, K. M. & Schrödl, M. New data from Monoplacophora and a carefully-curated dataset resolve molluscan relationships. *Sci. Rep.* **10**, 101 (2020).
4. Song, H. et al. Scaphopoda is the sister taxon to Bivalvia: evidence of ancient incomplete lineage sorting. *Proc. Natl Acad. Sci. USA* **120**, e2302361120 (2023).
5. Brusca, R. C., Moore, W. & Shuster, S. M. *Invertebrates* 3rd edn (Sinauer Associates, 2016).
6. Kobayashi, T. The Ancestory of the Cephalopoda from *Helcionella* to *Plectronoceras*. *Proc. Jpn Acad.* **63**, 135–138 (1987).
7. Mutvei, H. Restudy of some plectronocerid nautiloids (Cephalopoda) from the late Cambrian of China; discussion on nautiloid evolution and origin of the siphuncle. *GFF* **142**, 115–124 (2020).
8. Chen, J.-Y. & Teichert, C. Cambrian cephalopods from China. *Palaeontogr. Abt. A* **181**, 1–102 (1983).
9. Kröger, B. Cambrian-Ordovician cephalopod palaeogeography and diversity. *Geol. Soc. Lond. Mem.* **38**, 429–448 (2013).
10. Fang, X., Kröger, B., Zhang, Y.-D., Zhang, Y.-B. & Chen, T.-E. Palaeogeographic distribution and diversity of cephalopods during the Cambrian–Ordovician transition. *Palaeoworld* **28**, 51–57 (2019).
11. Pohle, A. et al. Early cephalopod evolution clarified through Bayesian phylogenetic inference. *BMC Biol.* **20**, 88 (2022).
12. Shigeno, S. et al. Evolution of the cephalopod head complex by assembly of multiple molluscan body parts: evidence from *Nautilus* embryonic development. *J. Morphol.* **269**, 1–17 (2008).
13. Yochelson, E. L., Flower, R. H. & Webers, G. F. The bearing of the new Late Cambrian monoplacophoran genus *Knightoconus* upon the origin of the Cephalopoda. *Lethaia* **6**, 275–309 (1973).
14. Webers, G. F. & Yochelson, E. L. Late Cambrian molluscan faunas and the origin of the Cephalopoda. *Geol. Soc. Lond. Spec. Pub.* **47**, 29–42 (1989).
15. Peel, J. S. The classes Tergomya and Helcionelloida, and early molluscan evolution. *Grønl. Geol. Unders. Bull.* **161**, 11–65 (1991).
16. Pojeta, J. & Runnegar, B. The paleontology of rostroconch molluscs and the early history of the phylum Mollusca. *US Geol. Surv. Prof. Pap.* **968**, 1–88 (1976).
17. Brock, G. A. & Paterson, J. R. A new species of *Tannuella* (Helcionellida, Mollusca) from the Early Cambrian of South Australia. *Mem. Ass. Aust. Palaeont.* **30**, 133–143 (2004).
18. Dzik, J. Brachiopod identity of the alleged monoplacophoran ancestors of cephalopods. *Malacologia* **52**, 97–113 (2010).
19. Dzik, J. Origin of the Cephalopoda. *Acta Palaeontol. Pol.* **26**, 161–191 (1981).
20. Moysiuk, J., Smith, M. R. & Caron, J.-B. Hyoliths are Palaeozoic lophophorates. *Nature* **541**, 394–397 (2017).
21. Sun, H.-J. et al. Hyoliths with pedicles illuminate the origin of the brachiopod body plan. *Proc. R. Soc. B* **285**, 20181780 (2018).
22. Liu, F., Skovsted, C. B., Topper, T. P., Zhang, Z.-F. & Shu, D.-G. Are hyoliths Palaeozoic lophophorates? *Natl Sci. Rev.* **7**, 453–469 (2020).
23. Li, L.-Y., Skovsted, C. B., Yun, H., Betts, M. J. & Zhang, X.-L. New insight into the soft anatomy and shell microstructures of early Cambrian orthothecids (Hyolitha). *Proc. R. Soc. B* **287**, 20201467 (2020).
24. Erwin, D. H. et al. The Cambrian conundrum: early divergence and later ecological success in the early history of animals. *Science* **334**, 1091–1097 (2011).
25. Kocot, K. M. et al. Phylogenomics reveals deep molluscan relationships. *Nature* **477**, 452–456 (2011).
26. Vinther, J. The origins of molluscs. *Palaeontology* **58**, 19–34 (2015).
27. Peterman, D. J., Landman, N. & Ciampaglio, C. Exploring the influence of cameral deposits on the stability, orientation, and maneuverability of orthocone cephalopods. *Paleobiology* **1**, 21 (2026).
28. Flower, R. H. *The Nautiloid Order Ellesmeroceratida (Cephalopoda)* (Socorro, 1964).
29. Teichert, C. *Main Features of Cephalopod Evolution* (Academic Press, 1988).
30. Hildenbrand, A., Austermann, G., Fuchs, D., Bengtson, P. & Stinnesbeck, W. A potential cephalopod from the early Cambrian of eastern Newfoundland, Canada. *Commun. Biol.* **4**, 388 (2021).
31. Landing, E., Kröger, B., Westrop, S. R. & Geyer, G. Proposed Early Cambrian cephalopods are chimaeras, the oldest known cephalopods are 30 m.y. younger. *Commun. Biol.* **6**, 32 (2023).
32. Smith, M. R. & Caron, J. B. Primitive soft-bodied cephalopods from the Cambrian. *Nature* **465**, 469–472 (2010).
33. Vinther, J. et al. A fossilized ventral ganglion reveals a chaetognath affinity for Cambrian nectocaridids. *Sci. Adv.* **11**, eadu6990 (2025).
34. Flower, R. H. *Cambrian Cephalopods* (New Mexico Bureau of Mines and Mineral Resources, 1954).
35. Kröger, B. The cephalopods of the Boda Limestone, Late Ordovician, of Dalarna, Sweden. *Eur. J. Taxon.* **41**, 1–110 (2013).
36. Sasaki, T., Shigeno, S. & Tanabe, K. *Anatomy of Living Nautilus: Reevaluation of Primitiveness and Comparison with Coleoidea* (Tokai Univ. Press, 2010).
37. Greenwald, L., Ward, P. & Greenwald, O. Cameral liquid transport and buoyancy control in chambered nautilus (*Nautilus macromphalus*). *Nature* **286**, 55–56 (1980).
38. Mutvei, H., Dunca, E. & Weitschat, W. Siphuncular structure in the Recent *Nautilus*, compared with that in Mesozoic nautilids and ammonoids from Madagascar. *GFF* **132**, 161–166 (2010).
39. Tanabe, K., Fukuda, Y. & Obata, I. Formation and function of the siphuncle-septal neck structures in two Mesozoic ammonites. *Trans. Proc. Paleontol. Soc. Jpn* **128**, 433–443 (1982).
40. Devaere, L. et al. Early Cambrian small shelly fossils from northwest Mexico: biostratigraphic implications for *Laurentia*. *Palaeontol. Electron.* **22**, 41A (2019).
41. Kouchisky, A. V. Skeletal microstructures of hyoliths from the Early Cambrian of Siberia. *Alcheringa* **24**, 65–81 (2000).
42. Sun, H.-J. et al. Periodic shell decollation as an ecology-driven strategy in the early Cambrian *Cupitheca*. *Palaeontology* **63**, 431–442 (2020).
43. Landing, E. & Kröger, B. Cephalopod ancestry and ecology of the hyolith "*Allatheca*" *degeeri* s.l. in the Cambrian Evolutionary Radiation. *Paleogeogr. Paleoclimatol. Paleoecol.* **353**, 21–30 (2012).
44. Martí Mus, M., Palacios, T. & Jensen, S. Size of the earliest mollusks: Did small helcionellids grow to become large adults? *Geology* **36**, 175–178 (2008).
45. Li, G.-X. et al. Early Cambrian metazoan fossil record of South China: generic diversity and radiation patterns. *Paleogeogr. Paleoclimatol. Paleoecol.* **254**, 229–249 (2007).
46. Budd, G. E. & Jackson, I. S. Ecological innovations in the Cambrian and the origins of the crown group phyla. *Phil. Trans. R. Soc. B* **371**, 20150287 (2016).
47. Skovsted, C. B. et al. The operculum and mode of life of the lower Cambrian hyolith *Cupitheca* from South Australia and North China. *Paleogeogr. Paleoclimatol. Paleoecol.* **443**, 123–130 (2016).
48. Liu, F. et al. Morphological disparity and evolutionary patterns of Cambrian hyoliths. *Pap. Palaeontol.* **10**, e1554 (2024).
49. Li, L.-Y. et al. Homologous shell microstructures in Cambrian hyoliths and molluscs. *Palaeontology* **62**, 515–532 (2019).
50. Qian, Y. Hyolitha and some problematica from the Lower Cambrian Meishucun stage in central and S. W. China. *Acta Palaeontol. Sin.* **16**, 255–275 (1977).
51. Parkhaev, P. Y. & Demidenko, Y. E. Zooproblematica and Mollusca from the Lower Cambrian Meishucun Section (Yunnan, China) and taxonomy and systematics of the Cambrian small shelly fossils of China. *Paleontol. J.* **44**, 883–1161 (2010).
52. Qian, Y., Xie, Y.-S. & He, T.-G. Hyoliths of the lower Cambrian Chiungchussuan Stage in south Shaanxi province. *Acta Palaeontol. Sin.* **40**, 31–43 (2001).
53. Yang, B., Steiner, M. & Keupp, H. Early Cambrian palaeobiogeography of the Zhenba–Fangxian Block (South China): independent terrane or part of the Yangtze Platform? *Gondwana Res.* **28**, 1543–1565 (2015).
54. Liu, F., Skovsted, C. B., Topper, T. P. & Zhang, Z.-F. A fresh look at the Hyolithid *Doliutheca* from the Early Cambrian (Stage 4) Shipai Formation of the Three Gorges Area, Hubei, South China. *Biology* **11**, 875 (2022).
55. Luo, J.-Z. et al. Resurgence of cloudinomorph fossils with possible cnidarian affinity at the peak of the Cambrian Explosion (Cambrian Series 2, Stage 3) in southern Shaanxi, China. *Pap. Palaeontol.* **10**, e1596 (2024).

Publisher's note Springer Nature remains neutral with regard to jurisdictional claims in published maps and institutional affiliations.

Springer Nature or its licensor (e.g. a society or other partner) holds exclusive rights to this article under a publishing agreement with the author(s) or other rightsholder(s); author self-archiving of the accepted manuscript version of this article is solely governed by the terms of such publishing agreement and applicable law.

© The Author(s), under exclusive licence to Springer Nature Limited 2026

Methods

Terminology

Morphological terminology follows established usage in studies of fossil and extant cephalopods[1,7,56]. Phylogenetic relationships within Mollusca are based on previously published hypotheses[3,4,11,23].

Material

Thirty-two three-dimensionally preserved, secondarily phosphatized specimens of *E. shaanxiense* gen. et sp. nov. were collected from the fourth site at the Liaoyeba section, Gaoqiao Town (GQ-LYB-4) in Zhenba County, Shaanxi Province, South China[57–59] (Extended Data Figs. 1 and 2). All fossils were recovered from phosphatic limestone in the Shuijingtuo Formation (Bed 1; Cambrian Stage 3[60,61]) (Extended Data Fig. 1). Rock samples were digested in 10% acetic acid, and the insoluble residues were washed, dried, and manually picked under a binocular microscope.

All examined specimens of *E. shaanxiense* gen. et sp. nov. are housed in the palaeontological collections of Chang'an University in Xi'an, Shaanxi Province, China. Specimen ID abbreviations are as follows: CU, Chang'an University; Bar, aluminium stub; BM, isolated septa imaged by ultra-deep-field microscopy; CT, uncoated specimens scanned using micro-CT.

Scanning electron microscopy

Specimens were sputter-coated with gold and imaged using the FEI Quanta 650 scanning electron microscope at Chang'an University in Xi'an, Shaanxi Province, China. This instrument is equipped with an Everhart–Thornley detector (ETD). Operating conditions were as follows: accelerating voltage = 15.0 kV; chamber pressure = 60 Pa; and working distance = 10.0 mm. Secondary electron images captured the surface ornament and outer shell wall layering; backscattered electron imaging was used selectively for compositional contrast.

Ultra-deep-field microscopy

Isolated septa were imaged with a Zeiss Smartzoom 5 ultra-deep-field microscope (Northwest University in Xi'an, Shaanxi Province, China) using high-transmission light. Images were acquired as stacked focal planes and digitally reconstructed to produce fully focused composites.

Micro-CT

Micro-CT scanning was performed on a single gold-coated specimen CUBar297-1 and two uncoated specimens CU(CT-Eoceras)−7 and CU(CT-Eoceras)−11, using the Zeiss Xradia 520 system at the State Key Laboratory of Continental Dynamics of Northwest University in Xi'an, Shaanxi Province, China. Scanning conditions were as follows: 40 kV accelerating voltage, 80 µA beam current, and an isotropic voxel size of 3.72 µm, 2.72 µm and 2.04 µm, respectively. Approximately 1,000 projection images were acquired in TIFF format. Data were reconstructed using standard, filtered back-projection algorithms and visualized in VG Studio Max 2.2 for three-dimensional volume rendering and segmentation. Supplementary Video 1 shows 3D view of shell and representative rendering of the internal segmented siphuncle.

Taphonomic criteria and preservation types

Three preservation modes were recognized: (I) phosphatized shell wall replicating the overall orthoconic shape of the phragmocone (Figs. 1a, 2a–e and 3 and Extended Data Fig. 3); (II) diagenetic phosphatic infillings of the camerae with thickened inter-cameral gaps (Fig. 2f–j); and (III) steinkerns of the siphuncle with relic septal junctions (Fig. 2k–m,o and Extended Data Fig. 4a–e).

Measurements and orientation

Shell length and width were measured in orthogonal SEM and micro-CT views to a precision of ±0.01 mm using CorelDRAW X7, and the measurement data were recorded in Microsoft Excel 2016. The expansion angle of the phragmocone was calculated as $\theta = 2\arctan\left(\frac{R_{\mathrm{aperture}} - R_{\mathrm{apex}}}{L}\right)$, where L is the measurable shell length and R_{aperture} is the maximum measurable radius of the aperture in transverse section and R_{apex} is the maximum measurable radius of the apex in transverse section. Tube-to-shell diameter ratios were measured at mid-segment positions. Orientation terminology (dorsal/ventral and apertural/apical) follows previous studies[12,56]. Segment counts denote enclosed units divided from each other by septa; the flaring segment is the expanded terminal unit at the apertural end of the shell.

Statistics and reproducibility

SEM and micro-CT micrographs shown herein were selectively sampled from our fossils specimen data to optimally showcase the diagnostic morphological features described. All key observations (for example, the presence of a probable siphuncle, the morphology of the septa and the presence of three outer shell layers) were confirmed on multiple specimens representing at least two different preservation types. Measurements were independently repeated by two authors; inter-observer variation was ≤5%. In addition, as a palaeontological investigation, this study relies on unique fossil specimens that constitute irreplaceable evolutionary record; such material cannot be experimentally replicated. Nonetheless, we supply comprehensive locality details and full methodological protocols to permit independent resampling of the fossil-bearing horizons and full reproducibility of all analytical workflows.

Reporting summary

Further information on research design is available in the Nature Portfolio Reporting Summary linked to this article.

Data availability

SEM data, ultra-deep-field microscopy data and micro-CT data are available within this paper and in Extended Data Figs. 1–6, Extended Data Table 1 and the Supplementary Information. All raw micro-CT volume data (TIFF stacks) and segmentation files are deposited in Dryad (https://doi.org/10.5061/dryad.qbzkh18zk (ref. 62)). SEM images data of the three additional specimens (CUBar298-1, CUBar337-2 and CUBar297-5) listed in the measurement table (Extended Data Table 1) are available from the corresponding author upon reasonable request. The nomenclature of *E. shaanxiense* gen. et sp. nov. is registered in ZooBank (urn:lsid:zoobank.org:act:9916C67D-B5BC-418B-8E71-04166FDA3191 for genus and urn:lsid:zoobank.org:act:53734DFD-AF6C-43F2-96B7-4D2C73A5D877 for species). The Life Sciences Identifier for this publication is urn:lsid:zoobank.org:pub:F73274DC-5FD4-4130-A8E5-6E20B55AAFC2.

Code availability

No custom code was used in this study.

56. Teichert, C. et al. *Treatise on Invertebrate Paleontology*, *Part K* (Geological Society of America and Univ. of Kansas Press, 1964).
57. Li, Z.-C. et al. Petrogenesis and tectonic setting of the early middle Triassic subduction-related granite in the eastern segment of East Kunlun: evidences from petrology, geochemistry, and zircon U-Pb-Hf isotopes. *Int. Geol. Rev.* **64**, 698–721 (2022).
58. Zhao, L.-M. et al. Geochemical and zircon U-Pb-Hf isotopic study of volcanic rocks from the Yaolinghe Group, South Qinling orogenic belt, China: constraints on the assembly and breakup of Rodinia. *Precambrian Res.* **371**, 106603 (2022).
59. Ma, S.-J. et al. Provenance analysis of the Nanhua System in the Zhenba Xiaoyangba area, southern Shaanxi: evidence from detrital zircon U-Pb ages, clastic composition analysis and geochemistry. *Miner. Explor.* **15**, 165–189 (2024).
60. Dai, T., Zhang, X.-L. & Peng, S.-C. Morphology and development of the eodiscoid trilobite *Tsunyidiscus yanjiazhaiensis* from the Cambrian (Stage 3, Series 2) of South China. *J. Syst. Palaeontol.* **14**, 75–89 (2016).
61. Zhang, X.-G. & Clarkson, E. N. K. Phosphatized eodiscoid trilobites from the Cambrian of China. *Palaeontogr. Abt. A* **297**, 1–121 (2012).

62. Song, Z.-C. et al. *Eoceras* supplemental data from: Earliest siphuncle-bearing cephalopod from the early Cambrian. *Dryad* https://doi.org/10.5061/dryad.qbzkh18zk (2026).

Acknowledgements We thank L. Y. Li for valuable suggestions; H. L. Lyu for sample collection in the field; D. H. Yang for artistic reconstructions; Y. R. Liu for assistance with SEM imaging; and J. Sun and Q. Zhang for assistance with micro-CT and ultra-deep-field microscopy, respectively.

Author contributions J.G., Z.S., J.H. and G.L. conceived the research. X.P. and J.G. led the fieldwork. J.P., Z.S., Y.Q., B.Z. and X.Z. collected rock and fossil samples. Z.S., J.G. and H.W. coordinated the project. Z.S. and B.P. drafted the manuscript with input from all authors. J.V., H.V.I., J.G., J.H. and G.L. revised the manuscript. All authors discussed the results and approved the final version.

Funding This study was supported by the National Natural Science Foundation of China (grants 42402011 to Z.S., 42172016 to J.G., 42372012 to J.H. and 42472044 to B.P.), the National Key Research and Development Program of China (grant 2023YFF0803601 to J.H. and G.L.), and the Opening Foundation of the State Key Laboratory of Continental Evolution and Early Life (grant 24LCD04 to J.G.).

Competing interests The authors declare no competing interests.

Additional information

Supplementary information The online version contains supplementary material available at https://doi.org/10.1038/s41586-026-10868-y.

Correspondence and requests for materials should be addressed to Junfeng Guo, Jakob Vinther or Hanjie Wen.

Peer review information *Nature* thanks Dirk Fuchs, Björn Kröger and the other, anonymous, reviewers for their contribution to the peer review of this work. Peer reviewer reports are available.

Reprints and permissions information is available at http://www.nature.com/reprints.

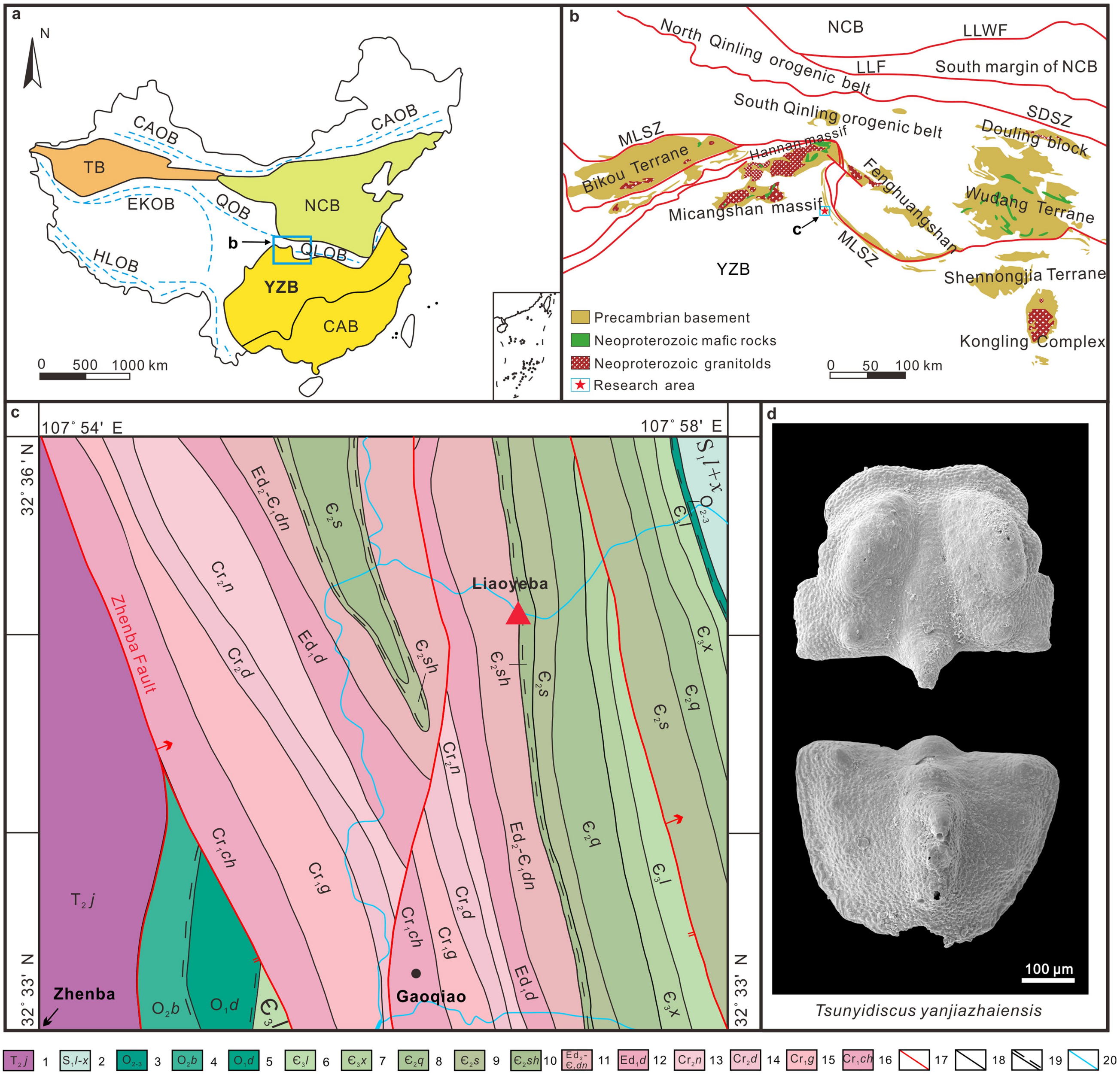
a
N
CAOB
CAOB
TB
EKOB
QOB
NCB
b
QLOB
HLOB
YZB
CAB
0 500 1000 km
b
NCB
LLWF
North Qinling orogenic belt
LLF
South margin of NCB
South Qinling orogenic belt
SDSZ
MLSZ
Hannan massif
Douling block
Bikou Terrane
Fenghuangshan
Wudang Terrane
Micangshan massif
c
MLSZ
YZB
Shennongjia Terrane
Precambrian basement
Neoproterozoic mafic rocks
Neoproterozoic granitolds
Research area
Kongling Complex
0 50 100 km
c
107° 54′ E
107° 58′ E
32° 36′ N
32° 33′ N
32° 33′ N
Zhenba Fault
Liaoyeba
Gaoqiao
Zhenba
T₂j
O₂b
O₁d
Ed₂-Є₁dn
Є₂s
Є₂sh
Cr₂n
Cr₂d
Cr₁g
Cr₁ch
Ed₁d
Є₂q
Є₃x
Є₃l
S₁l+x
O₂₋₃
d
100 μm
Tsunyidiscus yanjiazhaiensis
T₂j 1
S₁l-x 2
O₂₋₃ 3
O₂b 4
O₁d 5
Є₃l 6
Є₃x 7
Є₂q 8
Є₂s 9
Є₂sh 10
Ed₂-Є₁dn 11
Ed₁d 12
Cr₂n 13
Cr₂d 14
Cr₁g 15
Cr₁ch 16
17
18
19
20

Extended Data Fig. 1 | Geological setting of the Cambrian Series 2 Shuijingtuo Formation in the Liaoyeba section, Gaoqiao Town, Zhenba County, Shaanxi Province. a, Simplified tectonic map, showing the study area on the northern margin of the Yangtze Block. Adapted with permission from ref. 57, Taylor & Francis. **b**, Schematic geological framework, showing the study area situated adjacent to the Micangshan and Hannan massifs. Adapted with permission from ref. 58, Elsevier. **c**, Geological map of the Zhenba area, showing strata ranging in age from Cryogenian to Triassic. Adapted with permission from ref. 59, Mineral Exploration. **d**, Cranidium and pygidium of the trilobite *Tsunyidiscus yanjiazhaiensis*[60], which co-occurs with *E. shaanxiense* gen. et sp. nov. in the Shuijingtuo Formation (specimens CUBar306 [GQ-LYB-3]-7 and CUBar306 [GQ-LYB-3]-104) and therefore demonstrates that *E. shaanxiense* gen. et sp. nov. is restricted to Cambrian Stage 3[61]. Abbreviations: LLWF, Lingbo–Lushan–Wuyang Fault; LLF, Luonan–Luanchuan Fault; MLSZ, Mianlue Suture Zone; NCB, North China Block; QLOB, Qinling Orogenic Belt; QOB, Qilian Orogenic Belt; SDSZ, Shangdan Suture Zone; YZB, Yangtze Block. Stratigraphic units: 1, Lower Triassic Jialinjiang Formation; 2, Lower Silurian Xintan and Longmaxi formations; 3, Upper Ordovician Wufeng, Middle Ordovician Baota formations; 4, Middle Ordovician Baota Formation; 5, Lower Ordovician Dawan Formation; 6, Miaolingian Loushanguan Formation; 7, Miaolingian Xiwangmiao Formation; 8, Cambrian Series 2 Qingxudong Formation; 9, Cambrian Series 2 Shipai Formation; 10, Cambrian Series 2 Shuijingtuo Formation; 11, Ediacaran–Cambrian Dengying Formation; 12, Ediacaran Doushantuo Formation; 13, Cryogenian Nantuo Formation; 14, Cryogenian Datangpo Formation; 15, Cryogenian Gucheng Formation; 16, Cryogenian Chang'an Formation; 17, fault; 18, stratigraphic boundary; 19, parallel unconformity; 20, river. Red triangle marks the Liaoyeba section.

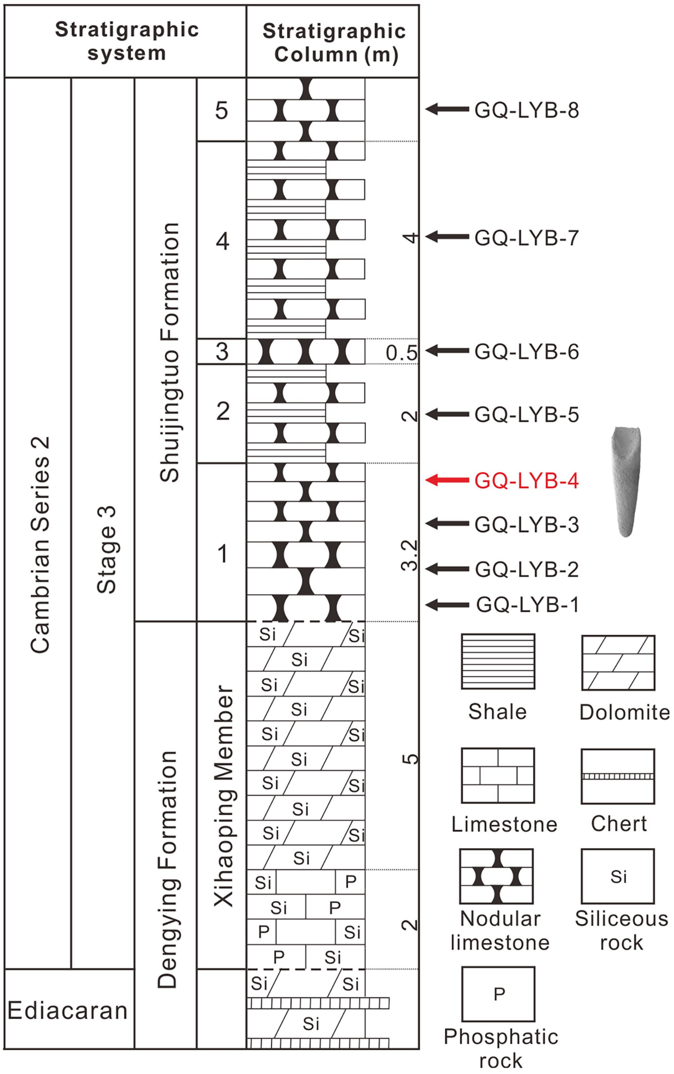
Stratigraphic system
Stratigraphic Column (m)
Cambrian Series 2
Stage 3
Shuijingtuo Formation
5
4
3
2
1
Ediacaran
Dengying Formation
Xihaoping Member
4
0.5
2
3.2
5
2
GQ-LYB-8
GQ-LYB-7
GQ-LYB-6
GQ-LYB-5
GQ-LYB-4
GQ-LYB-3
GQ-LYB-2
GQ-LYB-1
Si
P
Shale
Dolomite
Limestone
Chert
Nodular limestone
Siliceous rock
Phosphatic rock

Extended Data Fig. 2 | Stratigraphic column of the Liaoyeba section, Gaoqiao Town, Zhenba County, Shaanxi Province. Red arrow showing the horizon from which the specimens of *E. shaanxiense* gen. et sp. nov. were collected.

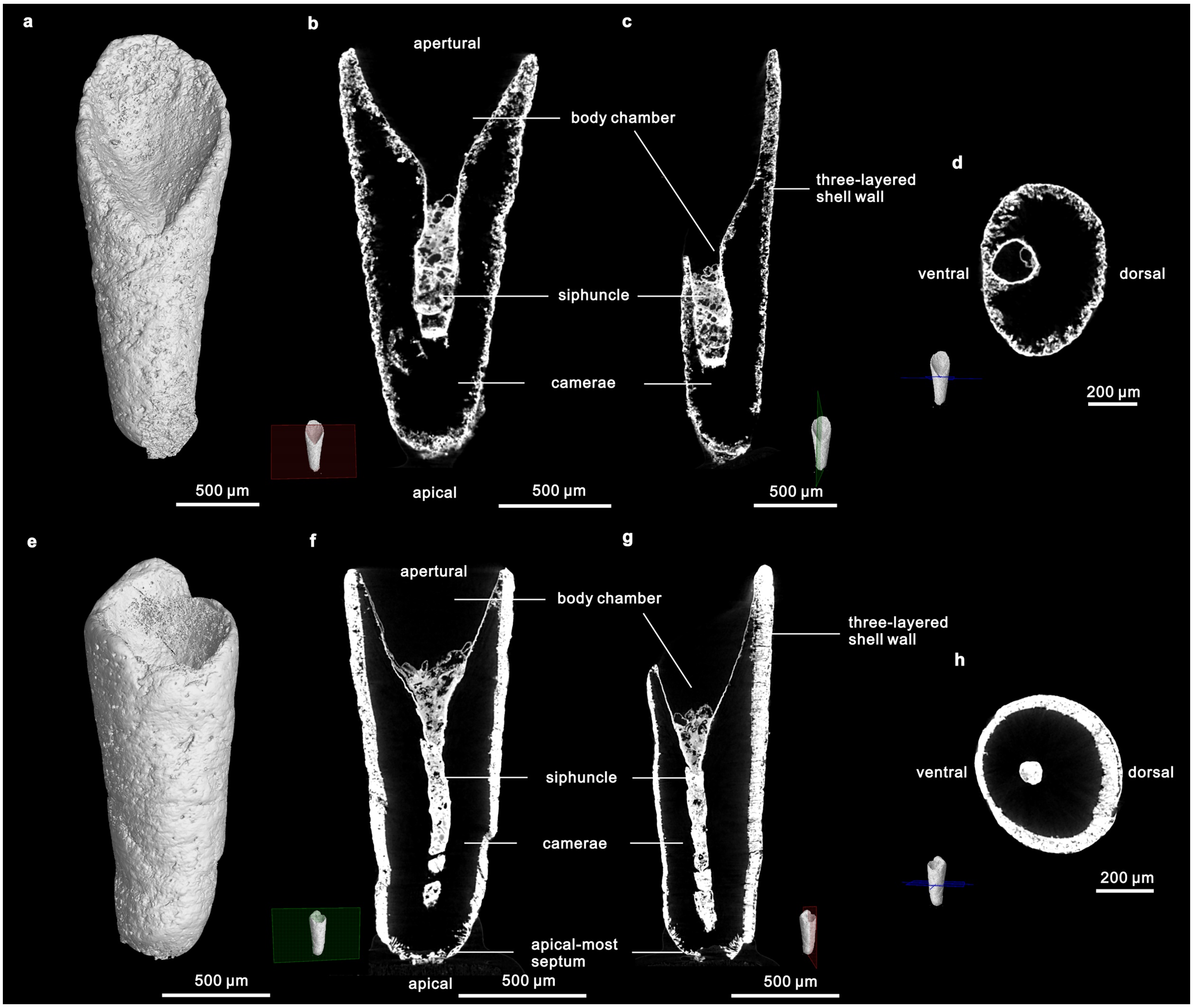
a
b
apertural
body chamber
c
three-layered
shell wall
d
ventral
dorsal
siphuncle
camerae
200 μm
500 μm
apical
500 μm
500 μm
e
f
apertural
body chamber
g
three-layered
shell wall
h
siphuncle
ventral
dorsal
camerae
200 μm
apical-most
septum
500 μm
apical
500 μm
500 μm

Extended Data Fig. 3 | Additional micro-computed tomography (micro-CT) images of *E. shaanxiense* gen. et sp. nov. a–d, CU(CT-Eoceras)-7. **e–h**, CU(CT-Eoceras)-11. **a**, **e**, ventral views of two secondarily phosphatized shells. **b**, **f**, median longitudinal sections. **c**, **g**, median tangential sections. **d**, **h**, median transverse sections. Together, the images display all the key morphological features of *E. shaanxiense* gen. et sp. nov.

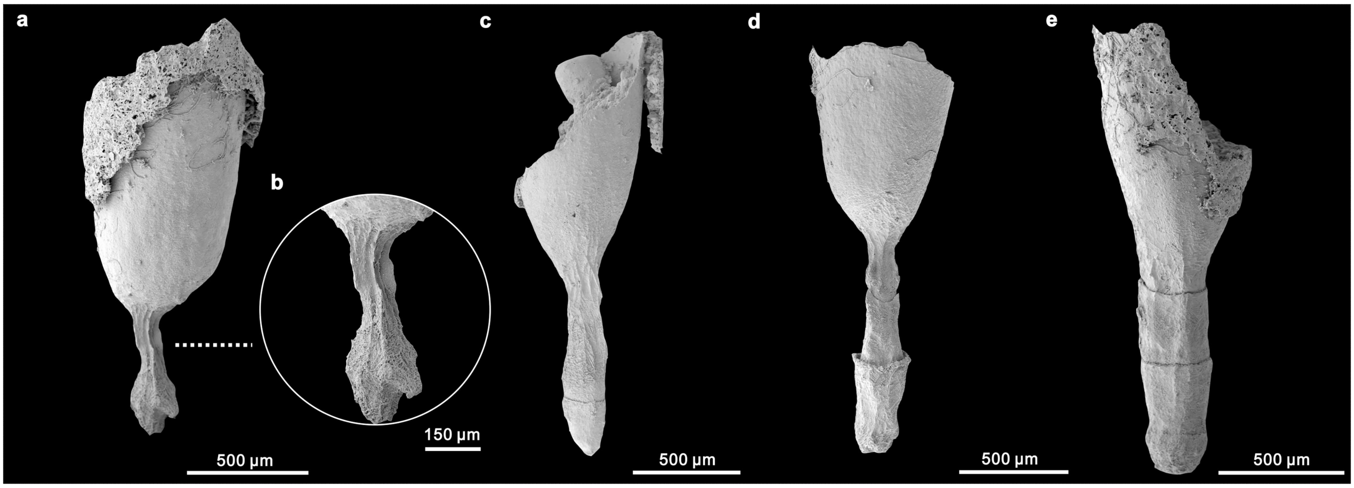

Extended Data Fig. 4 | Siphuncle development via mantle membrane condensation in *E. shaanxiense* gen. et sp. nov. a, b, CUBar299-9. **a**, Expansive, flaring mantle membrane narrowing distally into a siphuncle. **b**, Close-up of a, showing the succeeding shrunken body-siphuncle membrane structure with walls that were likely organic or weakly mineralized. **c**–**e**, CUBar335-17, CUBar299-25 and CUBar299-16, respectively, showing body chambers followed by different numbers of siphuncular segments.

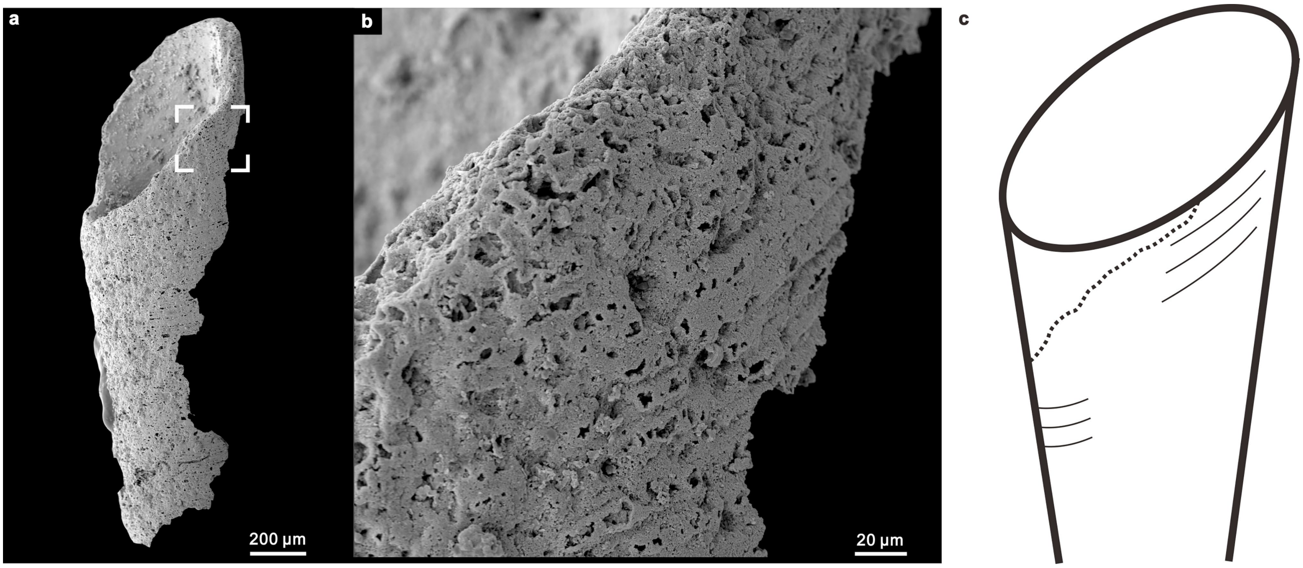

Extended Data Fig. 5 | Growth lines in the apertural region of *E. shaanxiense* gen. et sp. nov. a, **b**, CUBar300-9. **a**, Lateral view of a partial phragmocone. **b**, Close-up of the box in a, showing the fine external ribs (growth lines) aligned parallel to the oblique apertural margin. **c**, Simplified line drawing of *E. shaanxiense* gen. et sp. nov. in lateral view, showing the oblique growth lines in the apertural region and the transverse growth lines in the abapertural region. The dotted line indicates a possible line of breakage below the apertural margin.

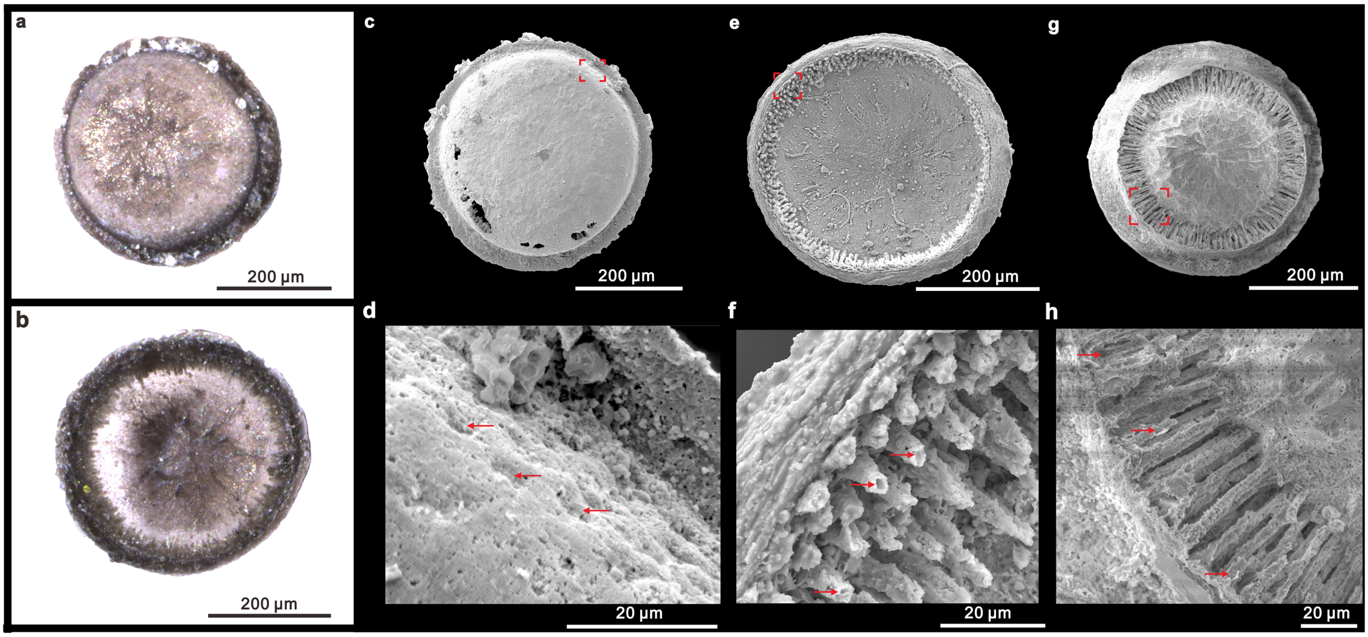

Extended Data Fig. 6 | Ultra-deep-field and scanning electron microscopy images of isolated septa of *E. shaanxiense* gen. et sp. nov. a, **b**, BM-05, apical and apertural views, respectively. Ultra-deep-field microscopy, showing the convex central portion and the planar marginal portion under intense illumination, and indicating that the central part is extremely thin and semi-transparent. **c**, CUBar301-3, apical view. SEM image, showing a complete septum preserving the convex central portion and the planar marginal portion. **d**, Close-up of the box in c, showing some of the pits (red arrows) on the transitional marginal corner. **e**, CUBar336-16, apertural view, showing relic canal structures corresponding to pits (red arrows) on the opposite side of the septum. **f**, Close-up of the box in e, showing some of the hollow canals within each prism (red arrows) on the transitional inner margin of the septum. **g**, CUBar301-31, apical view. Septum with broken central portion showing radial canals structures. **h**, Close-up of the box in g, showing hollow canals structures (red arrows) on the transitional marginal corner.

Extended Data Table 1 | Measurement on specimens of *E. shaanxiense* gen. et sp. nov

Specimens (CU, GQ-LYB-4)	Available length of shell (mm)	Available maximum diameter of shell (mm)	Available number of septa	Angle of expansion (°)	Preservation	Remarks
Bar297-1	3.5	0.9	4	15	Type I	Fig. 1a
Bar335-15	2.2	0.6	/	15		Fig. 2a
Bar297-4	3.5	0.8	/	12		Fig. 2b
Bar298-5	2.9	0.7	/	8		Fig. 2c
Bar337-7	3.7	0.9	/	11		Fig. 2d
Bar335-1	4.4	1.0	/	12		Fig. 2e
Bar293-3	2.5	0.8	4	12	Type II	Fig. 2f
Bar297-8	3.3	0.9	5?	10		Fig. 2g
Bar297-10	2.7	0.9	6	14		Fig. 2h
Bar297-19	2.1	0.7	5	10		Fig. 2i
Bar298-20	2.2	0.7	5	10		Fig. 2j
Bar293-2	2.3	0.9	4	10	Type I	Fig. 3a
Bar301-41	1.6	0.7	2	9		Fig. 3b
Bar297-12	1.7	0.7	2?	11		Fig. 3d
Bar300-2	1.5	0.9	1	/		Fig. 3j
Bar298-11	2.5	0.8	/	10	Type I	Additional specimens
Bar337-2	3.0	0.9	5	12	Type II	
Bar297-5	2.7	0.7	5	11		

The number of septa includes internal and apical-most exposed septa.

nature portfolio

Corresponding author(s): Junfeng Guo, Jakob Vinther, Hanjie Wen

Last updated by author(s): Jun 23, 2026

Reporting Summary

Nature Portfolio wishes to improve the reproducibility of the work that we publish. This form provides structure for consistency and transparency in reporting. For further information on Nature Portfolio policies, see our Editorial Policies and the Editorial Policy Checklist.

Statistics

For all statistical analyses, confirm that the following items are present in the figure legend, table legend, main text, or Methods section.

n/a	Confirmed	
☐	☒	The exact sample size (*n*) for each experimental group/condition, given as a discrete number and unit of measurement
☒	☐	A statement on whether measurements were taken from distinct samples or whether the same sample was measured repeatedly
☒	☐	The statistical test(s) used AND whether they are one- or two-sided *Only common tests should be described solely by name; describe more complex techniques in the Methods section.*
☒	☐	A description of all covariates tested
☒	☐	A description of any assumptions or corrections, such as tests of normality and adjustment for multiple comparisons
☒	☐	A full description of the statistical parameters including central tendency (e.g. means) or other basic estimates (e.g. regression coefficient) AND variation (e.g. standard deviation) or associated estimates of uncertainty (e.g. confidence intervals)
☒	☐	For null hypothesis testing, the test statistic (e.g. *F*, *t*, *r*) with confidence intervals, effect sizes, degrees of freedom and *P* value noted *Give P values as exact values whenever suitable.*
☒	☐	For Bayesian analysis, information on the choice of priors and Markov chain Monte Carlo settings
☒	☐	For hierarchical and complex designs, identification of the appropriate level for tests and full reporting of outcomes
☒	☐	Estimates of effect sizes (e.g. Cohen's *d*, Pearson's *r*), indicating how they were calculated

Our web collection on statistics for biologists contains articles on many of the points above.

Software and code

Policy information about availability of computer code

Data collection	CorelDRAW X7 for size measurement. Microsoft Excel 2016 for size data recording.
Data analysis	VG Studio Max 2.2 for µCT data visualisation, three-dimensional volume rendering and segmentation.

For manuscripts utilizing custom algorithms or software that are central to the research but not yet described in published literature, software must be made available to editors and reviewers. We strongly encourage code deposition in a community repository (e.g. GitHub). See the Nature Portfolio guidelines for submitting code & software for further information.

Data

Policy information about availability of data

All manuscripts must include a data availability statement. This statement should provide the following information, where applicable:

- Accession codes, unique identifiers, or web links for publicly available datasets
- A description of any restrictions on data availability
- For clinical datasets or third party data, please ensure that the statement adheres to our policy

Scanning electron microscopy data, Ultra-deep-field microscopy data and Micro-computed tomography data are available within this paper and in Extended Data Figs. 1–6, Extended Data Table 1 and the Supplementary Information. All raw micro-CT volume data (TIFF stacks) and segmentation files are deposited in the Dryad Digital Repository under accession number DOI:10.5061/dryad.qbzkh18zk. Supplementary video 1 is available as Supplementary Information. SEM images data of the three additional specimens (CUBar298-1, CUBar337-2, CUBar297-5) listed in measurement table are available from the corresponding author upon reasonable request.

Research involving human participants, their data, or biological material

Policy information about studies with human participants or human data. See also policy information about sex, gender (identity/presentation), and sexual orientation and race, ethnicity and racism.

Reporting on sex and gender	n/a
Reporting on race, ethnicity, or other socially relevant groupings	n/a
Population characteristics	n/a
Recruitment	n/a
Ethics oversight	n/a

Note that full information on the approval of the study protocol must also be provided in the manuscript.

Field-specific reporting

Please select the one below that is the best fit for your research. If you are not sure, read the appropriate sections before making your selection.

☐ Life sciences ☐ Behavioural & social sciences ☒ Ecological, evolutionary & environmental sciences

For a reference copy of the document with all sections, see nature.com/documents/nr-reporting-summary-flat.pdf

Ecological, evolutionary & environmental sciences study design

All studies must disclose on these points even when the disclosure is negative.

Study description	This study reports a tubular small shelly fossil from the early Cambrian of South China. Fossils were collected from the field. Morphology and anatomy of fossils were described and analyzed using scanning electron microscopy, ultra-deep-field microscopy and micro-computed tomography. Taxonomy and evolution were also discussed.
Research sample	Fossil specimens of Eoceras shaanxiense gen et. sp. nov. were recovered from the the early Cambrian (Cambrian Age 3) Shuijingtuo Formation of China. These specimens illustrate all the key taxonomic features of this species and reveal that Eoceras is a minute stem cephalopod.
Sampling strategy	Fossils were recovered through manual picking (with the aid of binocular microscopes) of the insoluble residue of ~10% buffered acetic acid digestions of limestone. All specimens of Eoceras (including three different preservation types) seen within samples were collected and studied.
Data collection	Fossil specimens were picked and sorted in glass slides and examined preliminarily with the aid of binocular microscopes. The well-preserved specimens were sputter-coated with gold and imaged with scanning electron microscopy, the most complete were characterized using micro-computed tomography and specific isolated specimens were imaged with ultra-deep-field microscope.
Timing and spatial scale	The rock samples were collected from Liaoyeba section in field seasons during 2022-2025. All the fossils were yield from a 3.2m-thick limestone in the lower part of Shuijingtuo Formation.
Data exclusions	No data was excluded.
Reproducibility	As a palaeontological investigation, this study relies on unique fossil specimens that constitute irreplaceable evolutionary record; such material cannot be experimentally replicated. Nonetheless, the localities that are the sources of these specimens were provided for anyone to resample. All key observations were confirmed on multiple specimens representing at least two different preservation types. Measurements were independently repeated by two authors; inter-observer variation was ≤5%.
Randomization	Randomization is not an applicable method in this palaeontological study of all known material of a species.
Blinding	Blinding is not an applicable method in this palaeontological study of all known material of a species.

Did the study involve field work? ☒ Yes ☐ No

Field work, collection and transport

Field conditions	Rocks were well-exposed along the riverbed and the fossiliferous limestones were excavated manually in the field. The Shuijingtuo Formation is exposed in an area with a mild and humid climate with an average high temperature of 21°C, an average low temperature of 10° and an average amount of rainfall of 1300 mm per year.
Location	Liaoyeba section, Zhenba, China: 32°35′11″N, 107°56′43″E, 902 m.
Access & import/export	All fossil specimens in this study were collected by the field group led by Chang'an University in compliance with all local, national and international laws. All collecting permissions were obtained before the collecting started. Any collecting in private land also obtained permissions from the land holder.
Disturbance	All rock samples was manually collected with minimal disturbance of the surrounding environment.

Reporting for specific materials, systems and methods

We require information from authors about some types of materials, experimental systems and methods used in many studies. Here, indicate whether each material, system or method listed is relevant to your study. If you are not sure if a list item applies to your research, read the appropriate section before selecting a response.

Materials & experimental systems

n/a	Involved in the study	
☒	☐	Antibodies
☒	☐	Eukaryotic cell lines
☐	☒	Palaeontology and archaeology
☒	☐	Animals and other organisms
☒	☐	Clinical data
☒	☐	Dual use research of concern
☒	☐	Plants

Methods

n/a	Involved in the study	
☒	☐	ChIP-seq
☒	☐	Flow cytometry
☒	☐	MRI-based neuroimaging

Palaeontology and Archaeology

Specimen provenance	All specimens were collected from the Shuijingtuo Formation, at the Liaoyeba section of Zhenba Country, Shaanxi Province, China.
Specimen deposition	All specimens are housed in the palaeontological collections of Chang'an University in Xi'an, Shaanxi Province, China.
Dating methods	No new dates are provided in this study.

☐ Tick this box to confirm that the raw and calibrated dates are available in the paper or in Supplementary Information.

Ethics oversight	No ethics permissions were required to undertake this study.

Note that full information on the approval of the study protocol must also be provided in the manuscript.

Plants

Seed stocks	n/a
Novel plant genotypes	n/a
Authentication	n/a